Supporting Information

An unprecedented pyridine-based dinuclear mixed-valent $Re^{I/VII}$ oxo-bridged complex: Solvatochromic and AIE-active probe for nanomolar detection of picric acid and trinitrotoluene

Atasi Mukherjee, Suman Bhattacharyya and Manab Chakravarty*

Details on the Studies:

Absorption and fluorescence studies

Stock solutions of 10^{-3} M **An-4Py** and **Re-4Py** were prepared in DMF. The absorption studies were performed by adding the sample (2 mL, 10^{-5} M) to a quartz cuvette (1 cm × 1 cm). Emission spectra were simultaneously recorded with the same sample used for absorption. The excitation wavelength was 405 nm with an excitation slit/emission slit of 5.0 and PMT voltage of 400 eV.

Aggregation-induced emission enhancement [AIE(E)] studies

AIE(E) studies were performed using a mixture of DMF and water. The concentration of the probe (10^{-5} M) was kept constant throughout the experiment by varying the ratio of DMF and water (v/v%). All sensing studies were carried out with this aggregate.

NAC quenching studies

The handling of explosives such as PA and TNT was done carefully with proper protection and on the milligram scale at room temperature. PA was solubilized in distilled water and others nitroaromatics were solubilized in tetrahydrofuran (HPLC grade) to obtain 10^{-2} M of stock solutions. At first, the absorption and emission spectra were recorded with the aggregate (f_w = 90%; with highest fluorescence intensity) followed by the addition of different NACs having a concentration of 10^{-4} M.

Time-resolved decay measurement

The solution state lifetime was measured with the aggregated **Re-4Py** (2 mL, 10^{-5} M) via pulse excitation of 405 nm and emission at 560 nm followed by the addition of 1 µL, 3 µL (+2 µL), 5 µL (+2 µL) and 20 µL of PA and TNT solution to the aggregated probe. The decay curves for **Re-4Py** and after the addition of PA and TNT were best-fitted via tri-exponential manner.

Detection limit calculation

A series of titrations were carried out for the detection of PA and TNT using **Re-4Py**. A graph is plotted taking the log of quencher concentration on the X-axis and the ratio of fluorescence intensities after addition of quencher and maximum fluorescence intensity quenched on the Y-axis. The antilog of the X intercept is considered to be the detection limit.

Calculation of the Stern–Volmer constant

The Stern–Volmer constant was calculated using the equation: $I_0/I = 1 + K_{SV}[Q]$, where I_0 is the emission intensity in the absence of quencher, I is the emission intensity in the presence of quencher, K_{SV} is the quenching constant and [Q] is the concentration of the quencher. The K_{SV} value was derived from the slope of I_0/I vs. [Q] plots.

Cyclic voltammetry (CV) study

CV measurement was carried out using Ag/AgCl and Pt wire as the reference electrode and counter electrode, respectively. **Re-4Py** coated film on ITO was used as a working electrode in a typical three electrode system. Tetrabutylammonium hexafluorophosphate (0.1 M) in acetonitrile was used as the electrolyte. The spectrum was recorded at room temperature under an inert atmosphere (N_2 gas).

Paper strip quenching study

The aggregate solution of **Re-4Py** (10 μL, 10^{-4} M) was drop-casted into Whatman filter paper (2 cm × 2 cm) and allowed to dry at 25 °C. The picture was captured after it dried completely. Then different concentrations of PA and TNT (5 μL) solution were dropped on the fluorescent probe and the image was taken after 1 min. However, the quenching was occurred immediately.

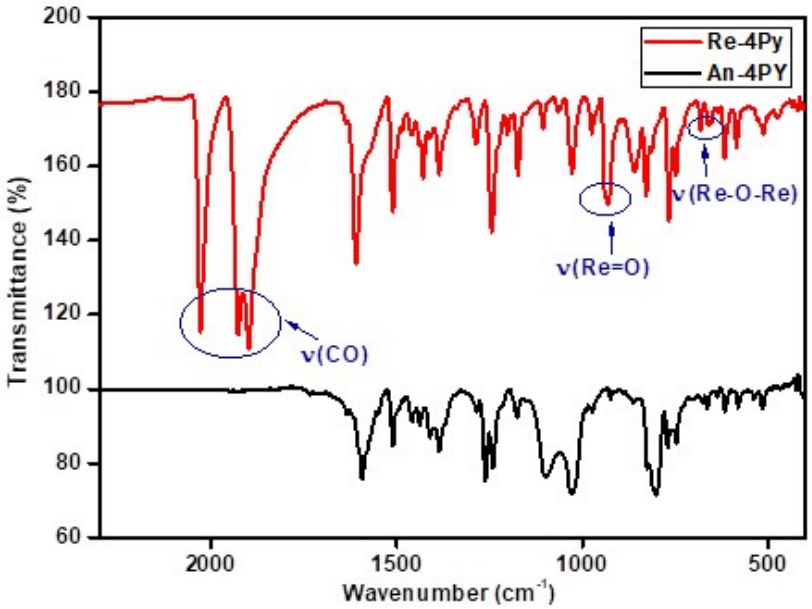

Figure S1. IR spectra of **An-4Py** and **Re-4Py**.

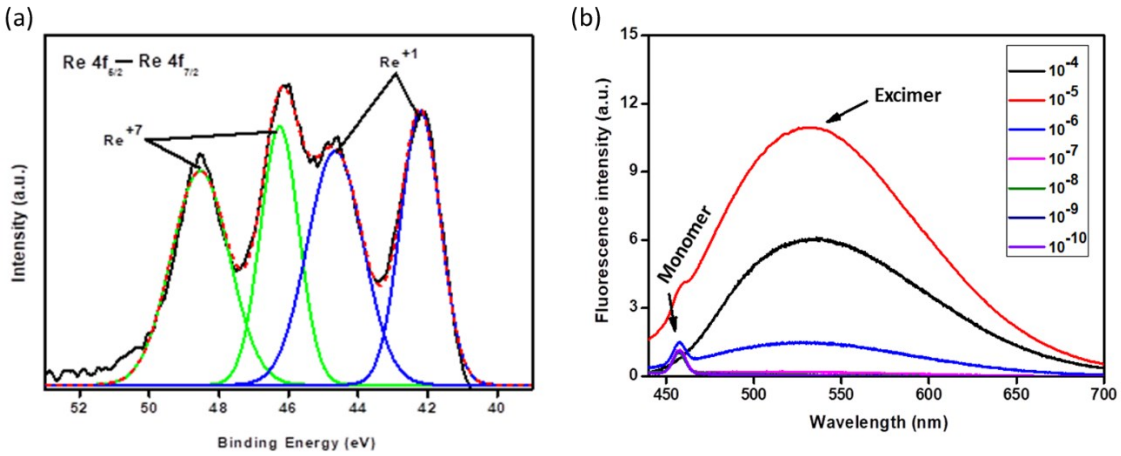

Figure S2. (a) XPS spectra of Re 4f region of **Re-4Py**. (b) Concentration-dependent emission spectra of **Re-4Py** in DMF.

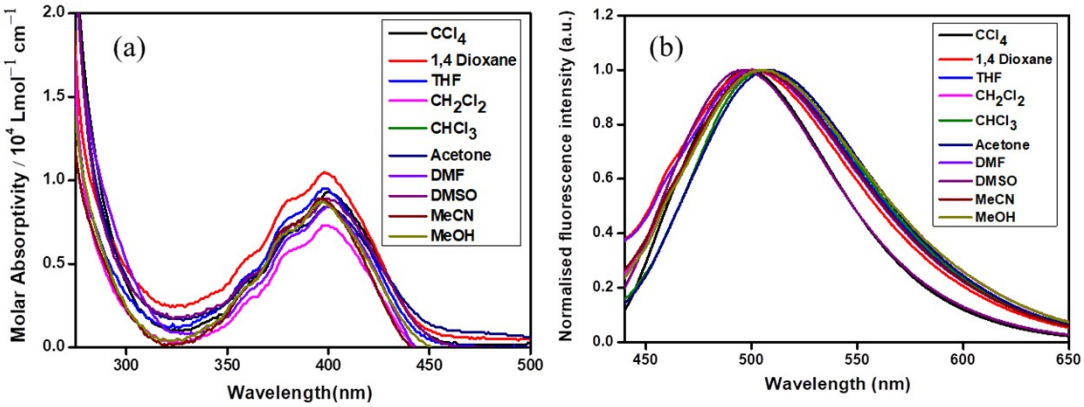

Figure S3. (a) Absorption and (b) emission spectra of **An-4Py** (10^{-5} M) in different solvents. λ_{ex}= 405 nm.

Table S1. Absorption and emission maxima, relative quantum yields (Φ_f in %) of **An-4Py** in different solvents. The error: ± 3%.

Solvents	**Abs λ_{max} (nm)**	**Emi λ_{max} (nm)**	**Φ_f (%)**
CCl_4	400	499	7.78
1,4-Dioxane	400	501	7.29
THF	399	504	6.67
CH_2Cl_2	400	504	1.96
$CHCl_3$	399	506	3.58
Acetone	399	507	2.67
DMF	400	502	3.51
DMSO	400	506	2.59
MeCN	395	504	1.25
MeOH	397	504	0.80

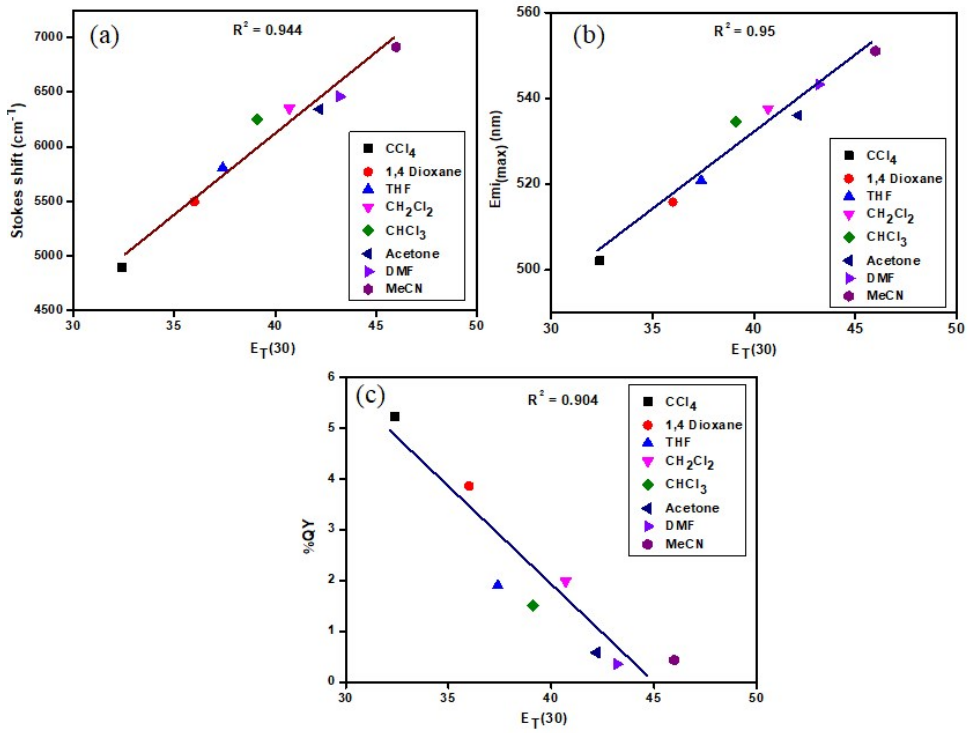

Figure S4. The plot of $E_T(30)$ vs. (a) Stokes shift, (b) Emission max (λ_{max}) and (c) quantum yield for **Re-4Py**. The error bar is ± 3%. The point for the solvent MeOH is neglected as it deviates significantly, possibly due to specific intermolecular interactions.

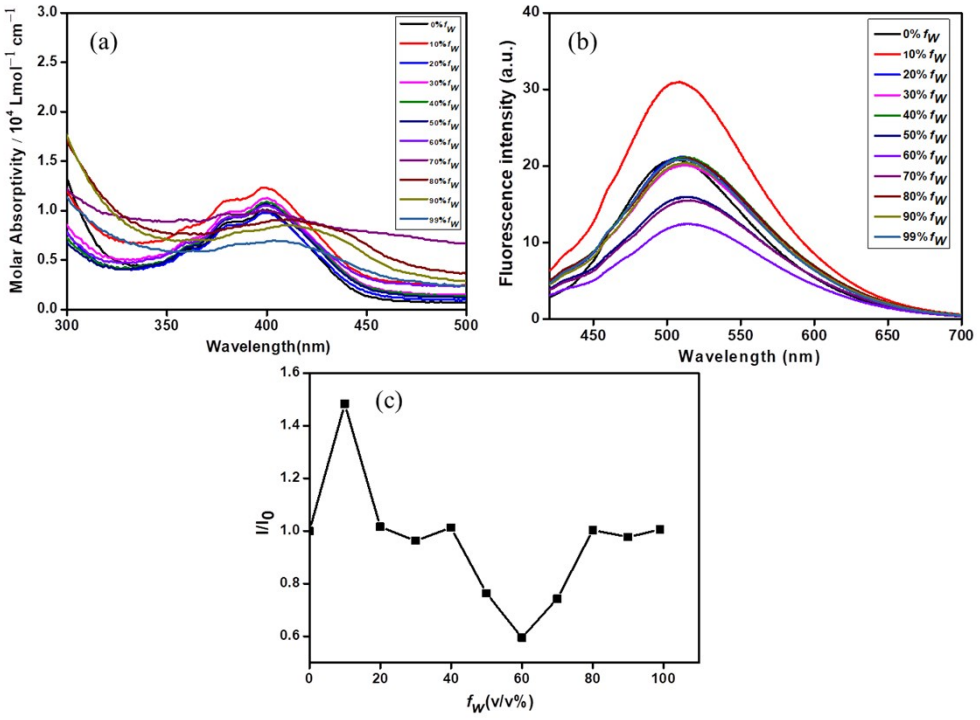

Figure S5. (a) Absorption and (b) emission spectra of **An-4Py** (10^{-5} M) with different f_w in DMF. (c) I/I_0 vs. f_w (v/v%). (I_0: initial intensity and I: intensity after the addition of water) λ_{ex}= 405 nm.

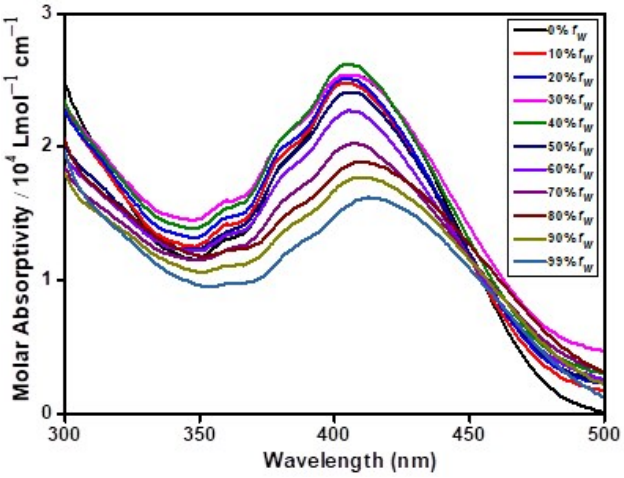

Figure S6. Absorption spectra of **Re-4Py** (10^{-5} M) with different f_w in DMF.

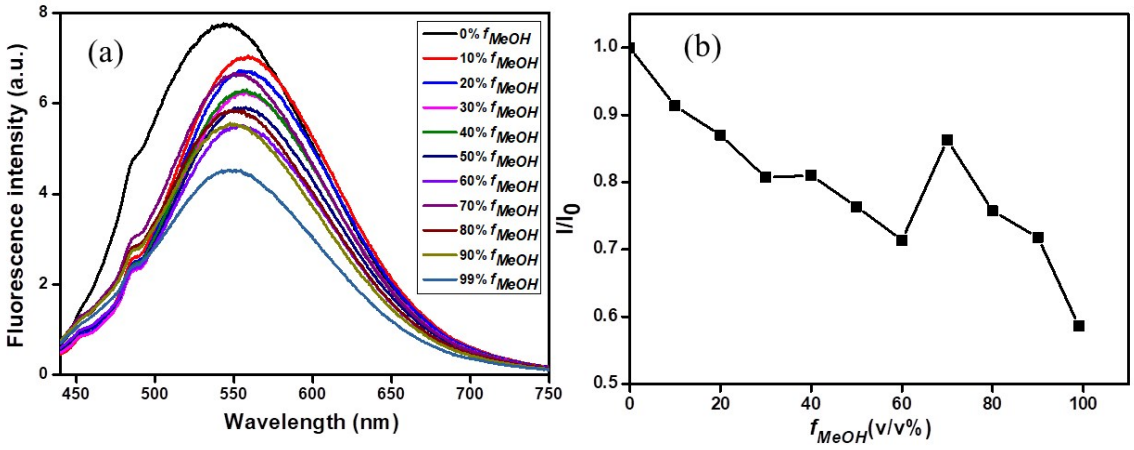

Figure S7. (a) Emission spectra of **Re-4Py** (10^{-5} M) with di□erent f_{MeOH} in DMF (b) I/I_0 vs f_{MeOH} (v/v %) (I_0: initial intensity and I: Intensity after addition of methanol) λ_{ex}= 405 nm.

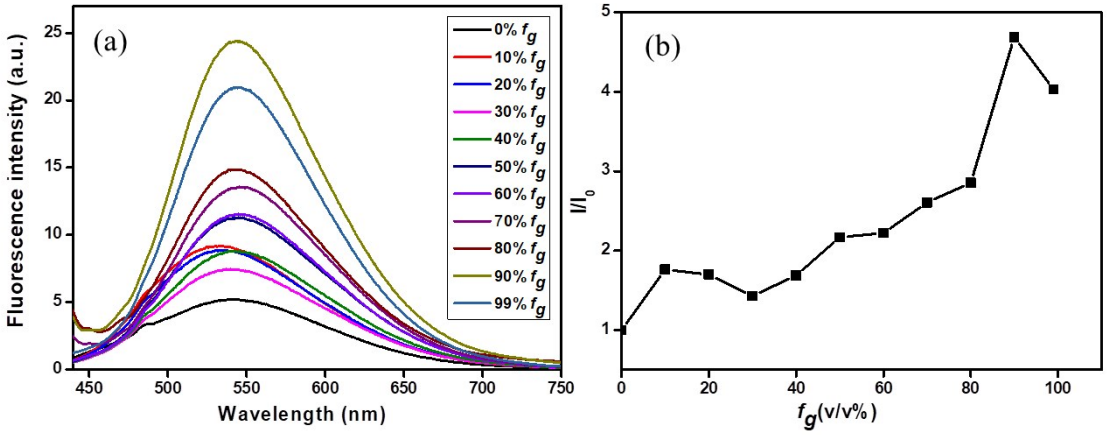

Figure S8. (a) Emission spectra of **Re-4Py** (10^{-5} M) with di□erent f_g in methanol (b) I/I_0 vs f_g (v/v %) (I_0: initial intensity and I: Intensity after addition of glycerol.) λ_{ex}= 405 nm.

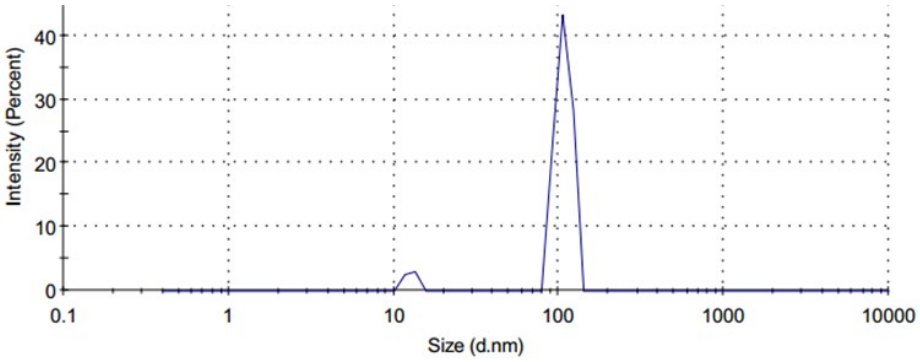

Figure S9. DLS plot of **Re-4Py** to find the average particle size.

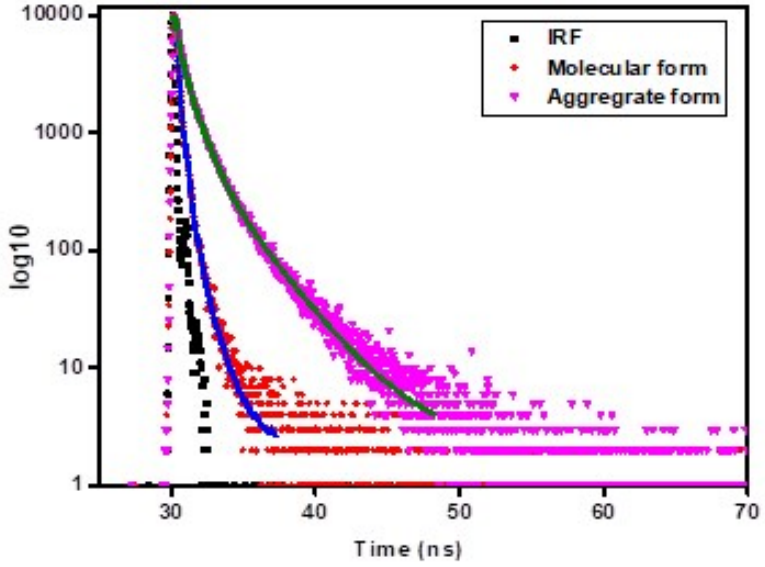

Figure S10. Lifetime decay plots of molecular and aggregate states of **Re-4Py**.

Table S2. k_r and k_{nr} values for **Re-4Py** in molecular and in aggregate states. $k_r = \Phi_f / \tau$, $k_r = (1-\Phi_f) / \tau$,

Form	Φ_f (%)	$\langle\tau\rangle$ (ns)	k_r (s^{-1})	k_{nr} (s^{-1})	k_r / k_{nr}
Molecular	0.35	0.92	3.80×10^{6}	1.08×10^{9}	3.52×10^{-3}
Aggregate	1.21	1.23	9.83×10^{6}	0.80×10^{9}	12.29×10^{-3}

Table S3. Life time data for **Re-4Py** in molecular and in aggregate states.

Form	α_1(%)	α_2(%)	α_3(%)	τ_1(ns)	τ_2(ns)	τ_3(ns)	<τ> (ns)	χ^2
Molecular	29.00	63.79	7.20	0.07	0.25	1.03	0.92	1.07
Aggregate	28.21	47.49	24.30	0.27	0.97	2.83	1.23	1.02

Table S4. Intermolecular Interactions in the ligand, **An-4Py** and complex **Re-4Py** (considering sum of van der Waals radii only)

Type of interactions	Distances (Å) for ligand (12)	Distances (Å) for complex (28)
C…H	2.867, 2.671, 2.761, 2.799, 2.824, 2.855,	2.897, 2.772, 2.870, 2.891, 2.799, 2.702, 2.442, 2.799, 2.888
H…H	2.286, 2.357, 2.371	1.901, 2.075, 2.130, 2.347, 2.252, 2.271
O…H	2.630	2.412, 2.603, 2.459, 2.619, 2.573 2.702, 2.650, 2.708
C…C	3.374	2.985 (not π…π)
N…H	2.721	
C…O		3.096, 3.173, 3.119, 3.102

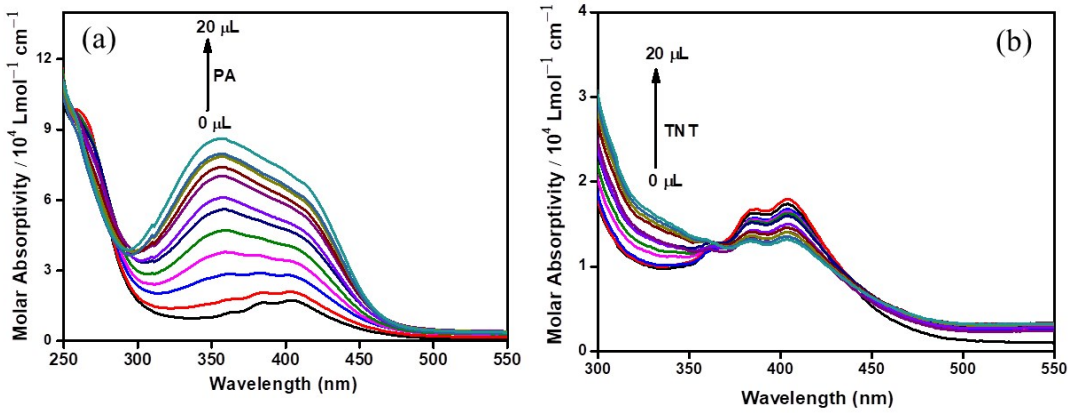

Figure S11. (a) Absorption spectra of aggregated **Re-4Py** upon the gradual addition of different volumes of (a) PA and (b) TNT solution (10^{-4} M).

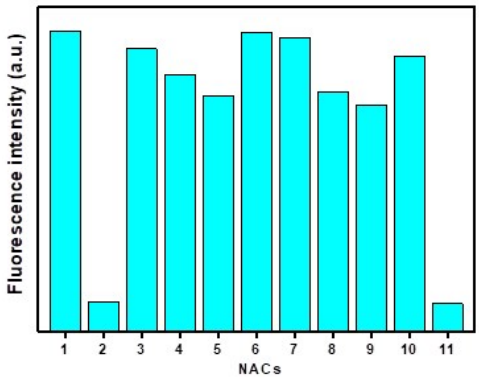

Figure S12. The bar diagram shows the quenching of PA in the presence of all other NACs (tested herein). The error: ± 3%. λ_{ex}= 405 nm. 1. Aggr.; 2. PA; 3. 2-NP; 4. 3-NAcP; 5. 3-NBAc; 6. 4-NBA; 7. Br-NB; 8. 4-NP; 9. NB; 10. 2-NAn; 11. PA + others.

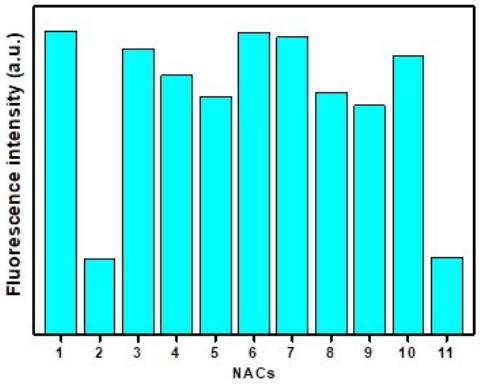

Figure S13. The bar diagram shows the quenching of TNT in the presence of all other NACs (tested herein). The error: ± 3%. λ_{ex}= 405 nm. 1. Aggr.; 2. TNT; 3. 2-NP; 4. 3-NAcP; 5. 3-NBAc; 6. 4-NBA; 7. Br-NB; 8. 4-NP; 9. NB; 10. 2-NAn; 11. TNT + others.

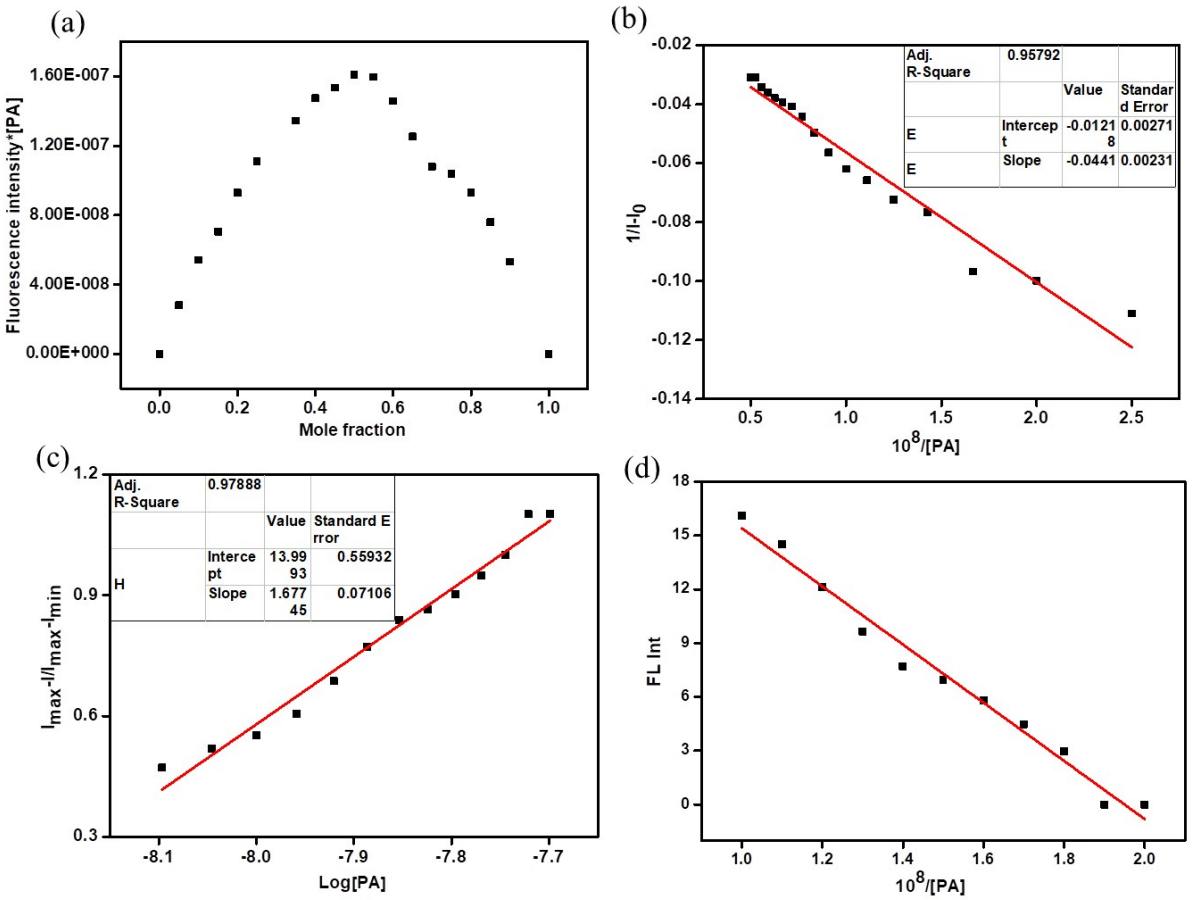

Figure S14. (a) Job's plot, (b) binding constant, (c) detection limit (method 1) and (d) detection limit (method 2) of aggregated **Re-4Py** for PA.

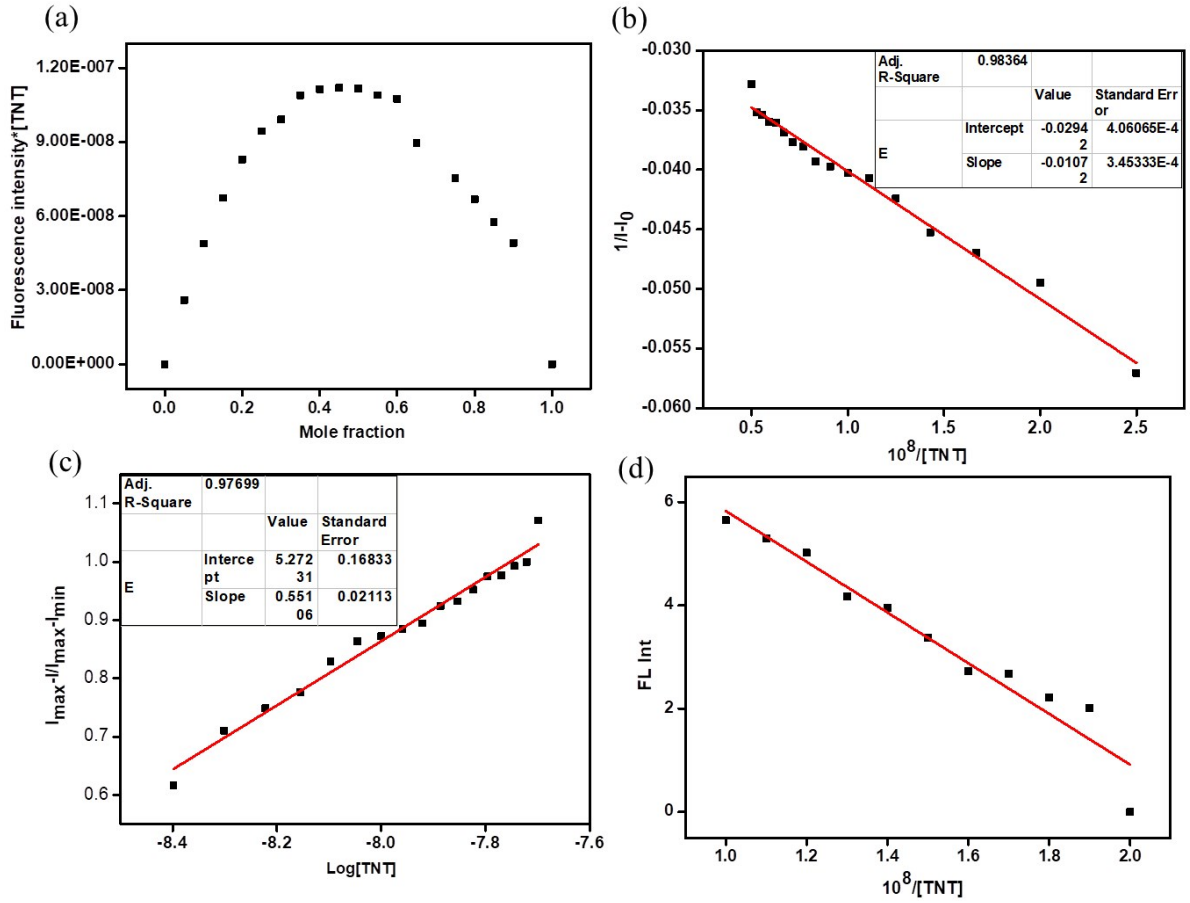

Figure S15 (a) Job's plot, (b) binding constant, (c) detection limit (method 1) and (d) detection limit (method 2) of aggregated **Re-4Py** for TNT.

Table S5. Comparison between previously reported probes to that of present work in terms of detection limit values for PA.

	S. No.	Description of probe	Detection limit in solution	Reference no. in the manuscript
PA	1	AIEE-active tripodal pyrazole compounds based on a 1,3,5-triethylbenzene scaffold	450 and 434 ppb	2(c)
	2	AIEE-active Alkoxy-Bridged Binuclear Rhenium(I) Complexes	--------	5(a)
	3	AIE-active Triphenylethylene-based biimidazole ligands and Re(I) complexes	8.2 x10^{-6} and 10.1x10^{-6} M,	13
	4	AIE-active hyperbranched polytriazole compounds	-------	17(a)
	6	AIEE-active pyreneamide-based compounds	0.13 pM	17(f)
	7	AIE-active pyridine-based dinuclear mixed-valent $Re^{I/VII}$ oxo-bridged complex	7.76x10^{-9} M	Present work

Table S6. Comparison between previously reported probes to that of present work in terms of detection limit values for TNT.

	S. No.	Description of probe	Detection limit in solution	Reference no. in the manuscript
TNT	1	AIPE-active iridium(III) bis(2-(2,4-difluorophenyl)pyridinato-*N,C2′*) (2-(2-pyridyl)benzimidazolato-*N,N′*) complex	9.08 mg mL^{-1}	17(c)
	2	AIE active hyperbranched polytriazole compounds	-------	17(a)
	3	AIEE-Active heterooligophenylene-based carbazole compounds	$30x10^{-9}$ and $40x10^{-9}$ mol L^{-1}	17(b)
	4	AIE-active anthracene-based electron-rich π-conjugate	$3.2x10^{-9}$ M	18(d)
	5	AIE active pyridine-based dinuclear mixed-valent $Re^{I/VII}$ oxo-bridged complex	$2.69x10^{-9}$ M	Present work

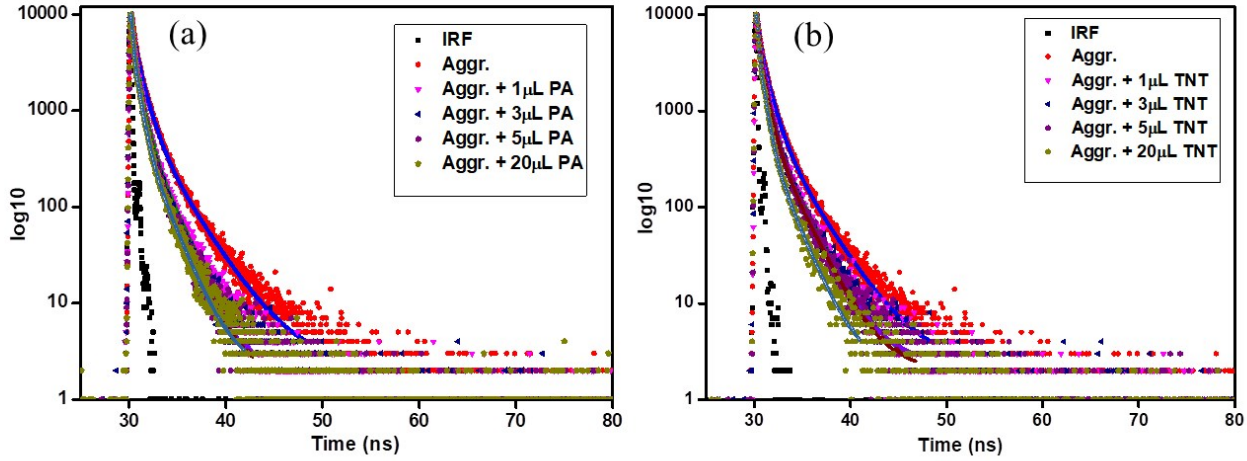

Figure S16. Lifetime decay plots of aggregated **Re-4Py** and after adding (a) PA and (b) TNT.

Table S7. Lifetime data for aggregated **Re-4Py** and after adding PA and TNT.

NACs	**Solution added (μL)**	α_1(%)	α_2(%)	α_3(%)	τ_1 (ns)	τ_2 (ns)	τ_3 (ns)	$\langle\tau\rangle$ (ns)	χ^2
	Only aggregate of **Re-4Py**	25.00	47.34	27.66	0.24	0.88	2.58	1.20	1.05
PA	1	33.52	42.36	24.12	0.18	0.63	1.94	0.79	1.02
	3	33.73	42.33	23.94	0.15	0.54	1.79	0.71	1.06
	5	36.77	42.34	20.89	0.15	0.59	1.88	0.70	1.08
	20	36.94	44.34	18.72	0.12	0.52	1.83	0.62	1.30
TNT	1	31.24	44.87	23.90	0.17	0.67	2.24	0.89	1.10
	3	33.88	44.56	21.56	0.17	0.69	2.24	0.85	1.01
	5	35.92	42.95	21.13	0.18	0.72	2.21	0.84	1.20
	20	34.84	44.07	21.09	0.14	0.54	1.77	0.66	1.13

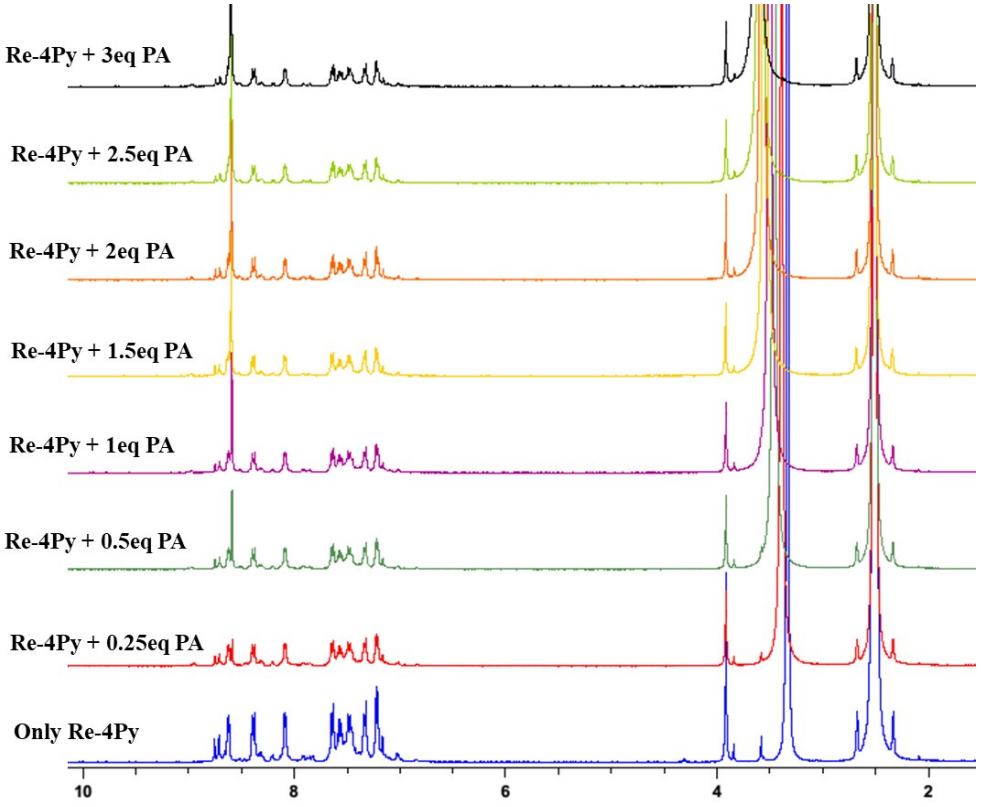

Figure S17. ^{1}H NMR spectra obtained for the titration of **Re-4PY** with PA in DMSO-d_6.

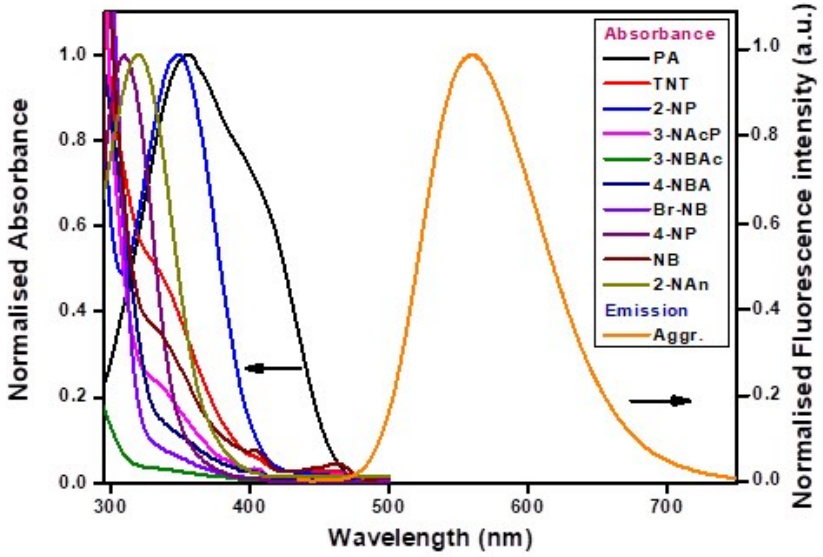

Figure S18. Absorption spectra of NACs (left) and emission spectrum of aggregated **Re-4Py** (right).

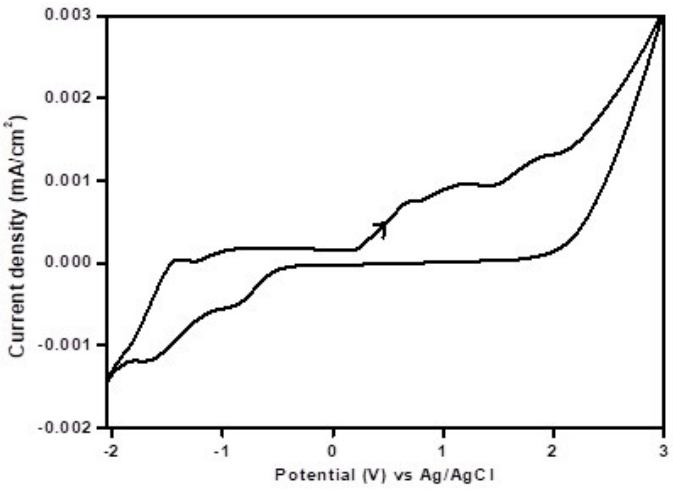

Figure S19. The cyclic voltammograms of **Re-4Py** (coated film on ITO) under inert atmosphere (N_2 gas) using Ag/AgCl as reference electrode. $E_{LUMO} = -(E_{onset}^{red} + 4.8 - 0.49)$ eV. [E_{onset}^{red} = -0.64 vs Ag/AgCl; E_{LUMO} = -3.67 eV]

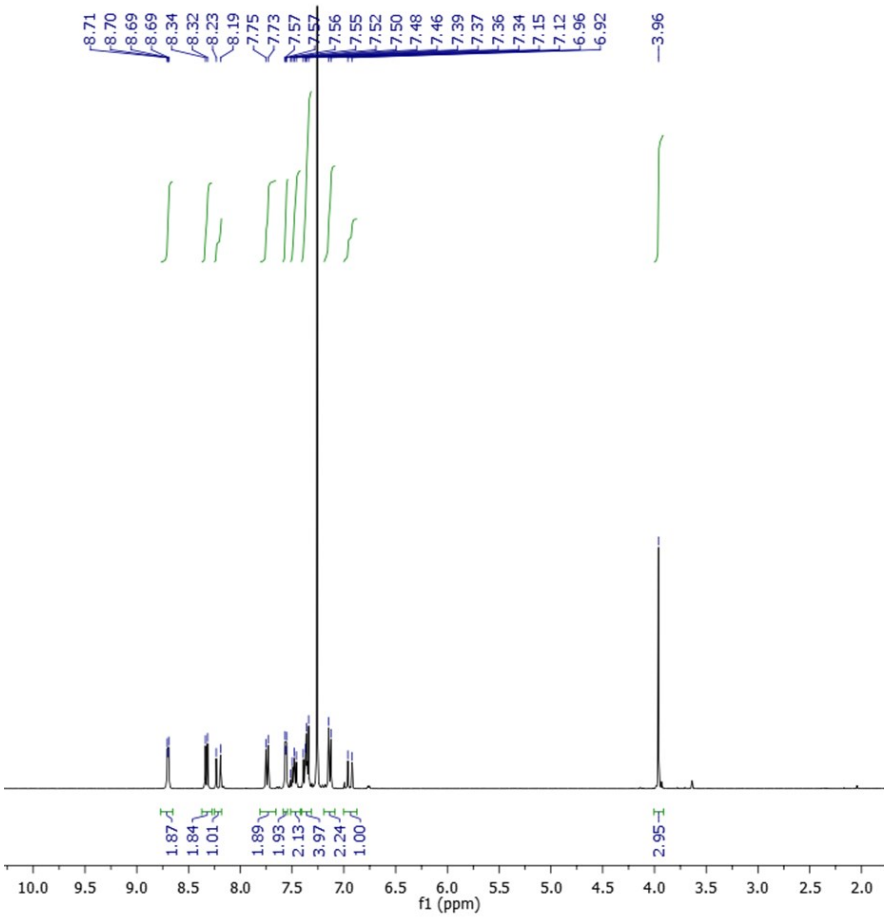

Figure S20. Partial ^{1}H NMR spectra of **An-4Py**.

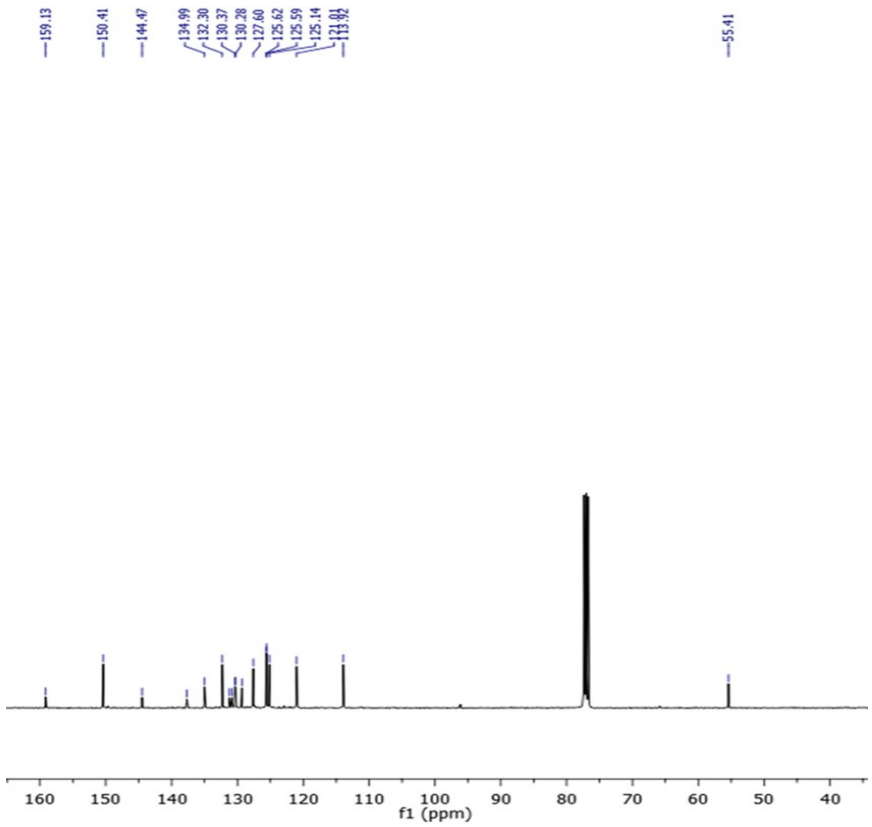

Figure S21. Partial ^{13}C NMR spectra of **An-4Py**.

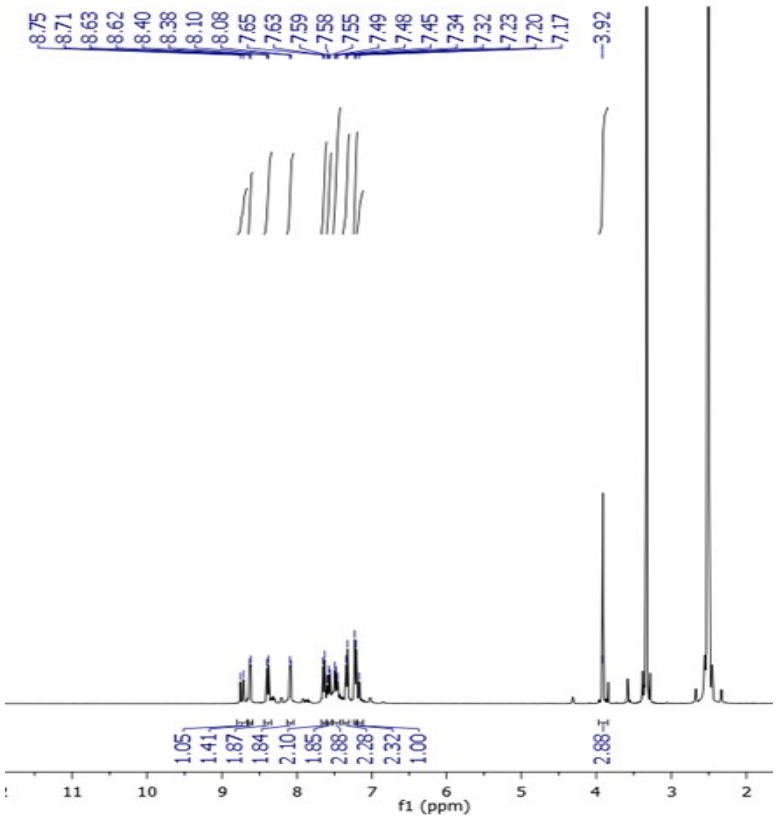

Figure S22. Partial ^{1}H NMR spectra of **Re-4Py**.

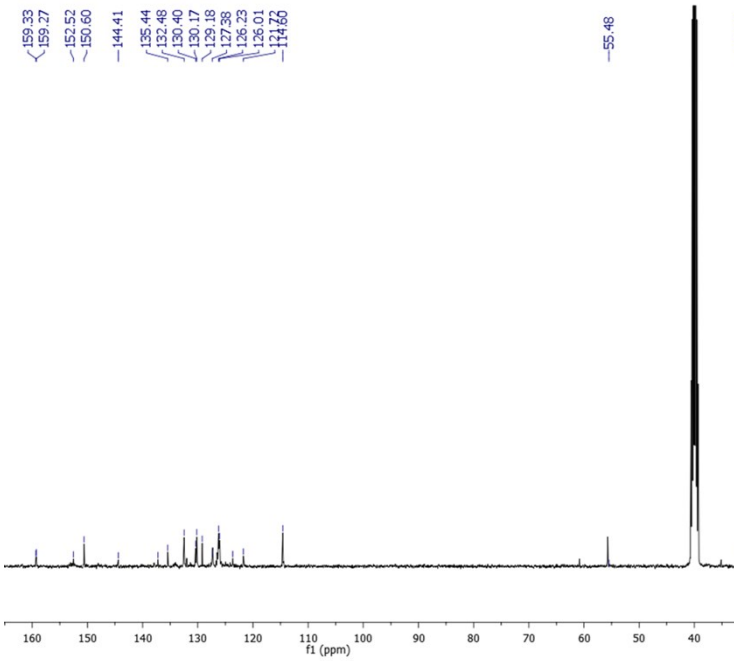

Figure S23. Partial ^{13}C NMR spectra of **Re-4Py**.

Compound Table

Compound Label	RT	Mass	Abund	Formula	Tgt Mass	Diff (ppm)
Cpd 1: 1.417 60.0441	1.417	1292.1875	163	C59 H42 N2 O9 Re2	1292.1949	-5.75

Compound Label	*m/z*	RT	Algorithm	Mass
Cpd 1: 1.417 60.0441	1318.1788	1.417	Find By Formula	1292.1875

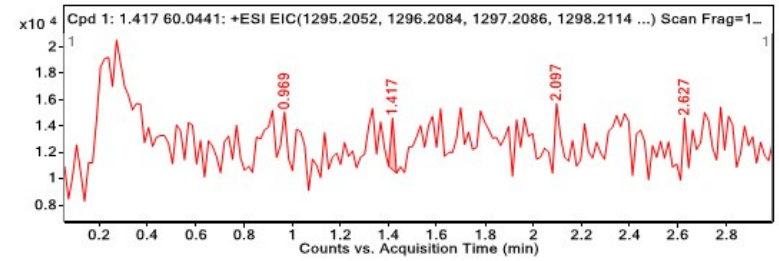

MS Zoomed Spectrum

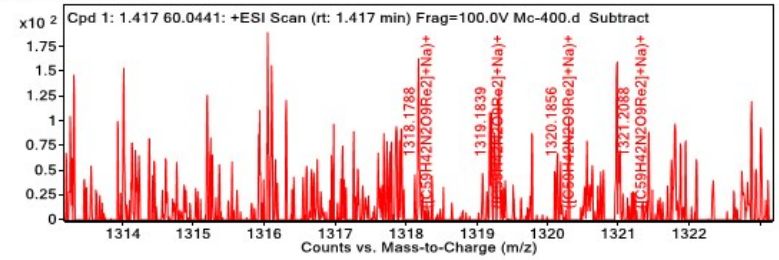

MS Spectrum Peak List

m/z	*Calc m/z*	Diff(ppm)	z	Abund	Formula	Ion
1318.1788	1318.1904	8.74	1	163.01	C59H42N2O9Re2	(M+Na)+
1319.1839	1319.1906	5.03	1	109.58	C59H42N2O9Re2	(M+Na)+
1320.1856	1320.1934	5.87	1	61.44	C59H42N2O9Re2	(M+Na)+
1321.2088	1321.1964	-9.4	1	30.11	C59H42N2O9Re2	(M+Na)+

Figure S24. HRMS spectra of **Re-4Py**.

END